



Seismic Behavior of Balloon Frame CLT Shear Walls with Different Ledgers

Md Shahnewaz¹; Carla Dickof²; and Thomas Tannert, M.ASCE³

Abstract: This paper presents experimental investigations on the seismic behavior of cross laminated timber (CLT) shear walls in a balloon frame configuration with various ledger assemblies attached at midheight. The tested system consisted of two seven-ply 191-mm-thick CLT panels with generic hold-downs, steel angle brackets, plywood surface splines, and nails as fasteners. A 2-story system was tested with a panel aspect ratio of 3:1 with different steel and wood ledgers under monotonic and quasistatic reversed cyclic loading. Three ledgers were subsequently tested under vertical quasistatic monotonic loading to determine their remaining load-carrying capacity. The tests showed that the shear wall displacement was due to the rocking of the wall panels, which themselves behaved as rigid bodies with negligible in-plane deformations. When compared to the monotonic tests, the strength in reversed cyclic tests was up to 21% lower. The ledger did not impede the desired rocking behavior of the wall, nor did the rocking of the wall reduce the remaining gravity load-carrying capacity of the ledgers by more than 7%. Balloon-framed CLT shear walls can be detailed and designed using the Canadian standard specifications for platform-type construction. DOI: [10.1061/\(ASCE\)ST.1943-541X.0003106](https://doi.org/10.1061/(ASCE)ST.1943-541X.0003106). © 2021 American Society of Civil Engineers.

Author keywords: Mass-timber; Cross-laminated timber (CLT); Balloon frame; Seismic design.

Introduction

Seismic Design Provisions for Cross-Laminated Timber Structures

Mass timber construction is becoming common across North America, and encapsulated mass timber structures have been incorporated into both the 2020 version of National Building Code of Canada (NBCC) for buildings up to 12 stories (NBCC 2020b) and the 2021 version of the International Building Code (IBC) for buildings up to 18 stories (ICC 2021). Cross-laminated timber (CLT) is a type of mass timber panel consisting of sawn lumber elements laid up on flat in alternating directions and glued together, creating panels that have high in-plane strength and stiffness (Shahnewaz et al. 2017; Karacabeyli and Gagnon 2019). Because of these properties, CLT can be used to resist lateral wind and seismic loads, in diaphragm or shear wall applications, and in earthquake-prone regions (Shahnewaz et al. 2018).

In Canada, the NBCC (2020b) defines ductility (R_d) and over-strength (R_o) factors for the reduction of seismic design forces and refers to the Standard for Engineering Design in Wood [CSA O86 (CSA 2019)] for design provisions for CLT shear walls and diaphragms. CSA O86 (CSA 2019) includes requirements intended to ensure that rocking is an energy dissipative kinematic wall behavior such as panel aspect ratio limitations and connection

design requirements. The NBCC-provided values of $R_d = 2.0$ and $R_o = 1.5$ are applicable where these requirements are met.

Platform-Framed CLT Shear Walls

These Canadian design provisions, developed based on CLT shear-walls and connection research (Hossain et al. 2016, 2019; Loss et al. 2018; Sullivan et al. 2018; Gavric et al. 2015a, b, c; Schneider et al. 2015; Trutalli et al. 2019; Popovski et al. 2010; Pozza et al. 2018), are applicable to platform-type construction. Platform-type construction has each floor act as a platform for the floor above; the wall system at each floor acts as an independent rocking wall system with connections to the floor below, as well as vertical joint connections between individual panels within the wall. Connections to the floor below are provided with brackets and hold-downs (HDs); wall panel connections typically use plywood splines or half-lap joints. Extensive research on the performance of CLT connections, including steel brackets, HDs, and self-tapping screws (STs), has demonstrated that both stiff and ductile connections can be achieved as a function of screw installation angle (Hossain et al. 2016, 2019; Loss et al. 2018), that spline joints achieved the largest ductility (Sullivan et al. 2018), and that brackets have similar strength and stiffness under tension and shear, whereas HDs showed higher strength and stiffness in tension when compared to bracket connections with negligible shear resistance (Gavric et al. 2015b, c; Schneider et al. 2015; Trutalli et al. 2019).

Other studies have developed design guidance to estimate the in-plane resistance and deflection of shear walls in platform-type CLT buildings (Popovski et al. 2010; Gavric et al. 2015a; Pozza et al. 2018; Shahnewaz et al. 2019, 2020a, b; Mestar et al. 2020; Izzi et al. 2018). Popovski et al. (2010) performed quasistatic monotonic tests with vertical shear connectors and demonstrated adequate seismic performance and ductile behavior. Gavric et al. (2015a) performed cyclic tests on coupled walls and observed that failure occurred at the connections, whereas the CLT panels only suffered negligible in-plane deformations. Pozza et al. (2018) presented a model for the behavior of CLT angle brackets under

¹Specialist Engineer, Fast+Epp, Vancouver, BC, Canada V5Y 1M2 (corresponding author). ORCID: <https://orcid.org/0000-0002-3814-8508>. Email: md.shahnewaz@alumni.ubc.ca

²Associate, Fast+Epp, Vancouver, BC, Canada V5Y 1M2. Email: cdickof@fastepp.com

³Professor, School of Engineering, Univ. of Northern British Columbia, Prince George, BC, Canada V2N 4Z9. Email: thomas.tannert@unbc.ca

Note. This manuscript was submitted on January 25, 2021; approved on April 16, 2021; published online on July 8, 2021. Discussion period open until December 8, 2021; separate discussions must be submitted for individual papers. This paper is part of the *Journal of Structural Engineering*, © ASCE, ISSN 0733-9445.

coupled shear tension and evaluated the model against experimental results. Other researchers proposed analytical models that predict the lateral behavior of CLT shear walls; for example, Shahnewaz et al. (2019, 2020a, b) proposed analytical methods to compute the resistance and deflection of single and coupled CLT shear walls considering different kinematic modes and the influence of perpendicular walls and ceiling. Mestar et al. (2020) developed an equivalent-frame model for CLT shear walls with openings and evaluated the performance under lateral loading. Izzi et al. (2018) reviewed the current state of the art of seismic performance of CLT structures. All these studies confirmed that the connections between CLT shear walls and the foundation and between panels were the primary contributors to deflection and ductility and supported the implementation of design provisions for platform-type CLT construction in standards around the world (Karacabeyli and Gagnon 2019).

Balloon-Framed CLT Shear Walls

The design provisions for CLT shear walls in CSA O86 (CSA 2019) apply only to platform-type construction, and the commentary goes on to note that balloon-type applications are beyond the scope of the standard. However, the code-specified aspect ratio limitations alongside platform framing significantly impact construction considerations because they increase both the number of panels that must be handled on site and the number of fasteners required between panels and floors. Additionally, for taller buildings, the limitations on flexural deformations can be difficult to achieve with HD deformations accumulating at each level. Finally, the accumulation of compression perpendicular to grain stresses on the floor panels from the stories above as well as shrinkage over multiple stories can be difficult to design for.

Conversely, balloon-type construction consists of continuous walls over multiple floors, with the intermediate floors framing into the face of each floor. Traditionally, balloon framing used continuous walls studs from the sill plate at the ground to the top plate at the roof of a building without interruption from floor framing. Although documentary evidence suggests that balloon framing existed as early as 1804 along the Mississippi River (Cavanagh 1997), George Snow is now commonly identified as the inventor of balloon-type construction, having built a warehouse on the bank of the Chicago River in 1832. From this modest beginning evolved a construction system that enabled the settlement of the treeless American West (Sprague 1981).

Balloon-framed CLT shear walls offer several advantages, including (1) eliminating perp-to-grain bearing between floors, (2) eliminating cumulative perp-to-grain shrinkage over the building height, (3) requiring fewer panels to create slender panel aspect ratios, (4) fewer HD and shear bracket connections are required over the height of a building, and (5) reduced flexural deformation, due to reduced cumulative deformation (Daneshvar et al. 2019). To date, however, only limited research is available on the seismic performance of balloon-type CLT construction. Chen and Popovski (2019) proposed mechanics-based analytical models to predict the lateral behavior of balloon-type CLT shear walls. They investigated the contribution of panel shear and bending as well as sliding, rocking, and slip of vertical joints to estimate the resistance and deflection of shear walls. CLT shear walls with dimensions of 4.1×0.8 m were tested in a single and coupled wall consisting of two segments. One monotonic and one cyclic test each were conducted with a nominal dead load applied; the lateral load was only applied at the top of the shear wall, and no ledgers simulating intermediate floors were attached, effectively testing a tall single-story wall. The actuator stroke was insufficient to achieve failure in the cyclic tests.

Objective

The structural consulting firm Fast+Epp proposed balloon-framed 2-story shear walls as a lateral load-resisting system for two elementary school projects. The objective of the research presented herein was to investigate the seismic behavior of this balloon CLT shear wall system with typical HDs and bracket base connectors and panel-to-panel spline connections designed to provide rocking behavior, similar to a platform framed system. Specific considerations include to determine the strength, stiffness, and energy dissipation of a rocking balloon frame wall system, including the impact of various ledger assemblies connected at midheight, and verification of the gravity load-carrying capacity of the ledgers after a seismic event.

Experimental Investigations

Specimen Description

A total of 12 CLT balloon-framed shear walls and subsequently six ledgers were tested in the UNBC Wood Innovation and Research Laboratory in Prince George, Canada. The test specimens consisted of two coupled CLT panels, 1,219 mm wide and 3,658 mm tall, resulting in an aspect ratio of 3:1, representing a half-scale 2-story shear wall; see Fig. 1. The test specimens consisted of two coupled CLT panels, 1,219 mm wide and 3,658 mm tall, resulting in an aspect ratio of 3:1, representing a half-scale 2-story shear wall, see Fig. 1. Only the panels were scaled to accommodate the laboratory test setup. All other parameters of the shear wall, such as the panel cross-section of the vertical loads, ledgers, and all connectors, were full size as designed for the actual building. This approach was deemed acceptable because previous research has shown the panel strength and stiffness contribution to shear wall resistance and deflection to be neglectable. The wall panels were connected to a steel beam using two HDs and four shear brackets on one side of the panels, and the steel beam was connected intermittently along its length to the lab's strong floor. The two panels were coupled vertically using a nailed plywood spline joint on one side.

Materials

The CLT panels were strength grade 191V2 [CSA O86 (CSA 2019)]: seven-ply, 191 mm thick ($35 + 17 + 35 + 17 + 35 + 17 + 35$), and sourced from Structurlam (CrossLam 2020). The shear walls were anchored on the outer edges to a steel beam with two WH740 HDs attached to the panel with $75 \text{ } 4\text{ } \times 60\text{-mm}$ anker nails; four TCN240 angle brackets—two on each panel—were attached with $36 \text{ } 4\text{ } \times 60\text{-mm}$ anker nails (Rothoblass 2020). The panel-to-panel vertical spline connections were provided with surface-mounted $25 \times 140\text{-mm}$ Douglas Fir (D.Fir) plywood pieces, spliced at one-third height of the wall and attached to the panel with $4\text{ } \times 60\text{-mm}$ anker nails at 200 mm on center with an one additional ASSYS Kombi $10\text{ } \times 120\text{-mm}$ screw (ASSY Kombi 2020) at the top and bottom of each piece of the spline. The predicted yield strength and deformation based on manufacturer values for HDs and brackets and fastener deformation calculations per EN 1995 (BSI 2004) for the splines were 106 kN and 101 mm, respectively.

Ledger Types

The CLT shear wall panels were balloon framed with a ledger attached at midheight to support the intermediate floor in the building. Four different ledger assemblies (see Fig. 2) were tested

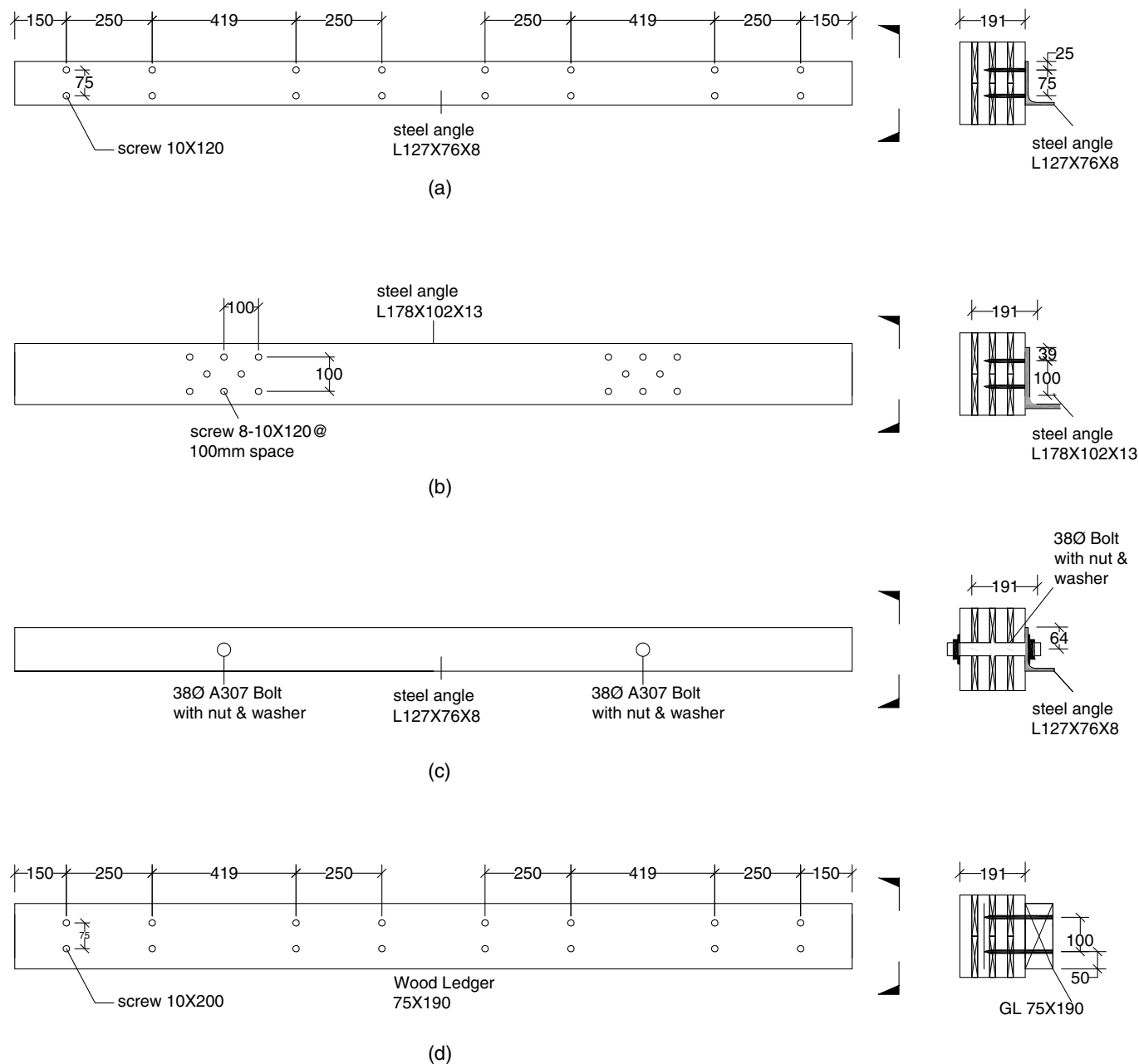


Fig. 2. Ledger assemblies: (a) Type A—steel with screws distributed; (b) Type B—steel with screws at centre; (c) Type C—steel with pin at centre; and (d) Type D—wood with distributed screws.

without imposing any restraint on the wall rocking behavior in addition to the friction between the two coupled panels and the friction created by the pin.

Type D—glulam GL75 × 190 ledger attached with 16 ASSY SK 10Ø × 200 partially threaded washer head screws distributed along the ledger length [Fig. 2(d)]. Type D is the same system as Type A ledger, except the ledger material is replaced with wood. The objective of using the wood ledger is to investigate its deformation and gravity load-carrying capacity due to reverse cyclic loading.

Setup for Shear Wall Tests

Each shear wall configuration with the different ledger types as described in Fig. 2 was tested three times: once under quasistatic

monotonic loading, to determine the displacement target for the subsequent two quasistatic reversed cyclic tests. Lateral loads were applied by two 250-kN actuators at the top of the wall panel through a steel side plate connected to a steel H-beam and at mid-height directly to the ledger. The top H-beam was placed on two wooden blocks at the center of each panel. These wooden blocks only served the purpose of spacers before the two large steel pins were inserted through which the superimposed dead loads were applied onto the panels. A 20-kN/m superimposed vertical gravity load was applied at the top of the wall representing a moderately loaded wall in a 2-story system. The load was applied using three cantilevered steel beams with weights on hollow structural sections (HSSs). This gravity load system simultaneously prevented out-of-plane horizontal movements in addition to allowing for the lateral movement of the shear wall. A three-dimensional

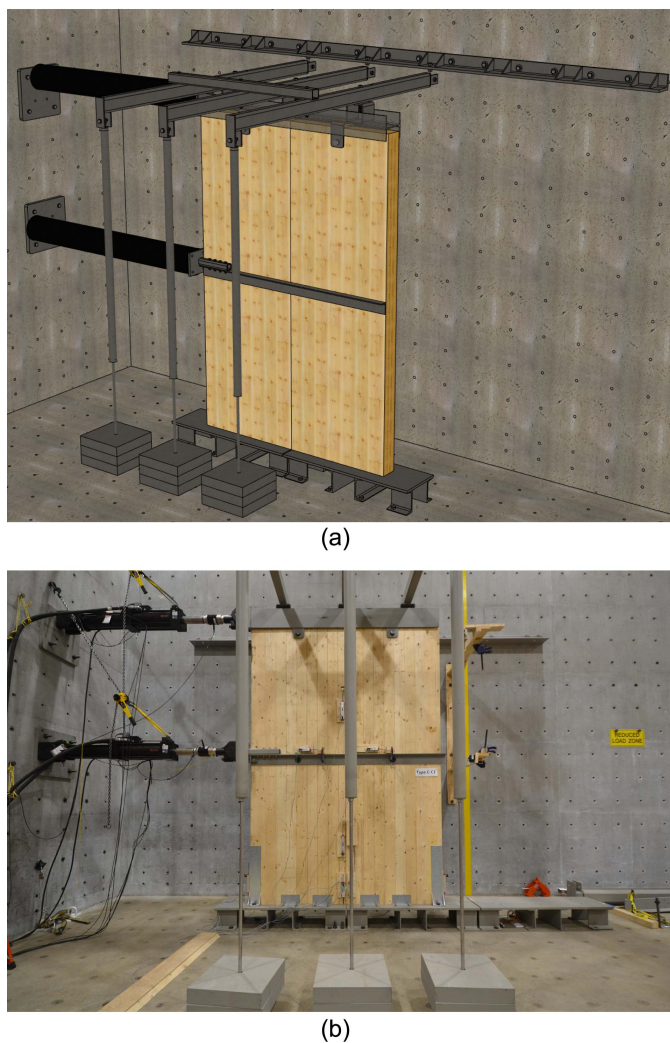


Fig. 3. (a) 3D schematic; and (b) photo of shear wall test setup.

(3D) schematic of the balloon wall test setup and a photo are shown in Fig. 3.

The balloon-framed shear walls were tested with a 20-kN/m superimposed vertical gravity load applied at the top of the wall. The test setup did not allow applying gravity loading onto the ledger; therefore, the setup did not entirely represent the actual loading situation in a balloon-framed building. However, we believe that this difference did not have any significant impact on the overall wall behavior. To evaluate the remaining gravity load-carrying capacity of the ledgers after a seismic event, the ledgers were retested only under gravity loading. Future numerical research can investigate the wall behavior with gravity loads applied at both story levels.

Instrumentation for Shear Wall Tests

The horizontal, vertical, and relative panel displacements were recorded with LVDTs and string pots at 12 locations (at the top and midheight of the wall, base, ledger, and spline), as shown in Fig. 4. Sensors 1 and 2 were string pots measuring the wall's horizontal displacements $d_{h,w}$. Sensors 3, 5, 6, and 8 were LVDTs measuring the vertical displacement between the testing apparatus and the bottom corner of each panel attached to record the uplifts $d_{up,w}$. Sensors 4 and 7 were LVDTs measuring the horizontal

displacement between the testing apparatus and the bottom center of each panel to record the horizontal wall sliding $d_{sl,w}$. Sensors 9 and 10 were LVDTs measuring the horizontal displacement between the ledger and the wall at the midpoint of each panel $d_{sl,l}$. Finally, Sensors 11 and 12 were LVDTs measuring the vertical slip between the coupled panels above and below the ledger $d_{z,p}$.

Loading Protocols

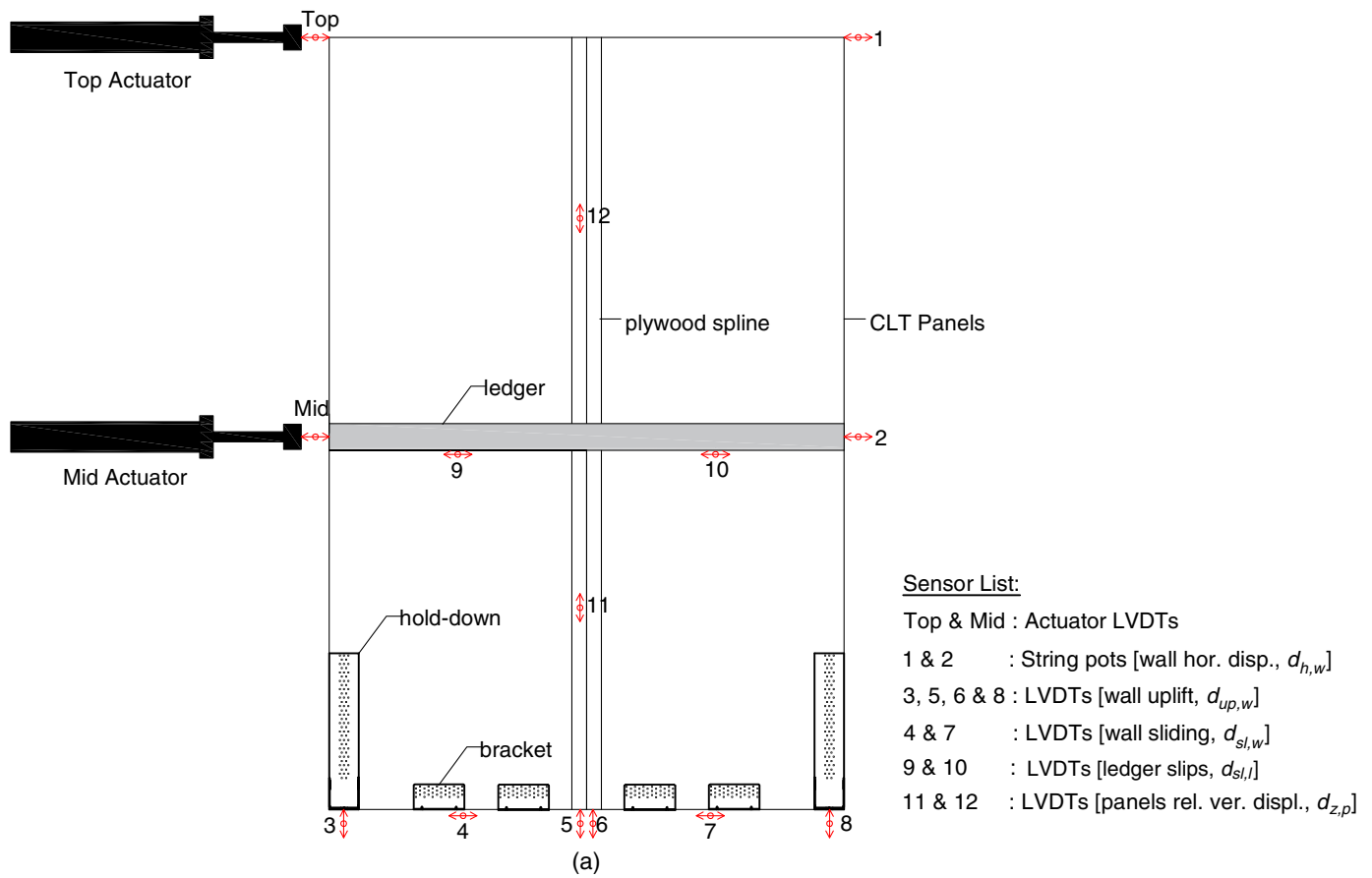
Based on the equivalent static analysis for story shears on a 2-story building, an approximation of equal forces acting at the roof and second level was deemed appropriate. To represent this loading in the experiments, both actuators applied the same load. The top actuator acted as the master and the midheight actuator as the slave trailing the top actuator's loads. The tests were conducted at a rate of 10 mm/min for the top actuator; the midheight actuator applied the same load directly to the ledger. In the quasistatic monotonic pushover tests, the shear walls were preloaded to 20 kN to validate the shear wall stiffness assumption. Tests were stopped at failure, defined as the point where the load-carrying capacity dropped to 80% of the maximum load. The reversed cyclic tests followed the abbreviated CUREE loading history [Fig. 5(a)], a displacement-controlled loading procedure per ASTM E2126 (ASTM 2011). The 100% target displacement for the cyclic loading tests was set to 60% of the observed displacement at failure from the monotonic tests.

Analysis of Shear Wall Tests

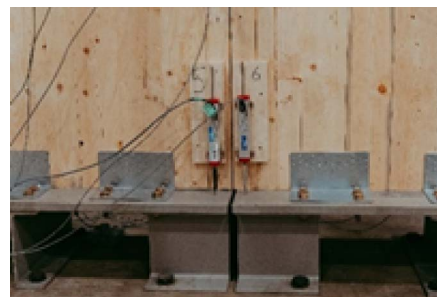
The shear walls tests were assessed in terms of strength, stiffness, deformation, ductility, and energy dissipation. The forces were presented as the sum of the two applied actuator loads. For the cyclic tests, both maximums from positive and negative cycles F_{max+} and F_{max-} were recorded. The deformations corresponding to the maximum forces d_{Fmax+} and d_{Fmax-} were the measurements at the top-right corner of the shear walls (Sensor 1 in Fig. 4). The other parameters, ultimate load (F_u), displacement at ultimate load (d_u), yield load (F_y), yield displacement (d_y), elastic stiffness (K_e), and ductility (D), were computed based on equivalent energy elastic plastic (EEEP) curves according to ASTM E2126. The elastic stiffness was calculated for the range of 10%–40% of capacity according to EN 26891 (CEN 1991). Ductility was computed as the ratio of displacement at ultimate to yield loads d_u/d_y , as outlined in ASTM E2126. Fig. 5(b) illustrates the procedure for developing the EEEP curves (created from the average of the positive and negative backbone curves). The energy dissipation E was calculated from the area under the loading and unloading cycles of the load-deflection hysteresis loops following the trapezoidal rule.

Ledger Tests

For shear walls with ledger types A, B, and D, the ledgers were subsequently tested under quasistatic monotonic loading as shown in Fig. 6 to determine the ledgers' remaining load-carrying capacity under gravity loading. Each of the three ledger types (A, B, and D) was tested twice: a control test (labeled "new") with the ledger not subjected to any loading prior to the monotonic shear connection test and a test on the ledger connection after the specimen was subjected to reversed cyclic loading tests (labeled "postseismic"). Ledger type C was not tested because there was no damage observed to the perfect pin. The ledger load displacement was recorded using the integrated actuator LVDTs. No external sensors were attached to the ledgers because the primary aim of these



(b)



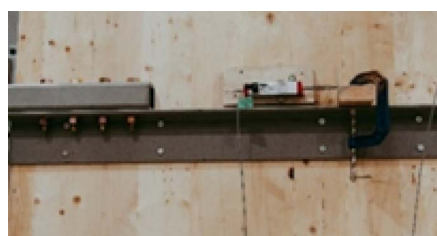
(c)



(d)



(e)



(f)



(g)

Fig. 4. Shear wall testing: (a) schematic; (b) end of wall uplift; (c) uplift at the inner panel edge; (d) panel sliding; (e) relative panel slips; (f) ledger slips; and (g) wall horizontal displacement.

tests was to investigate the remaining load capacity of the ledgers after the rocking shearwalls failed at their energy dissipating connections. The load-carrying capacities (F_{max}), displacement at capacities (d_{Fmax}) and elastic stiffness (K_e) were recorded. The stiffness K_e was calculated for the range of 10%–40% of capacity according to EN 26891 (CEN 1991).

Results and Discussion

Shear Wall Test Main Results

Key test results for the wall behavior are listed in Table 1. The load-displacement response from the monotonic and reversed cyclic

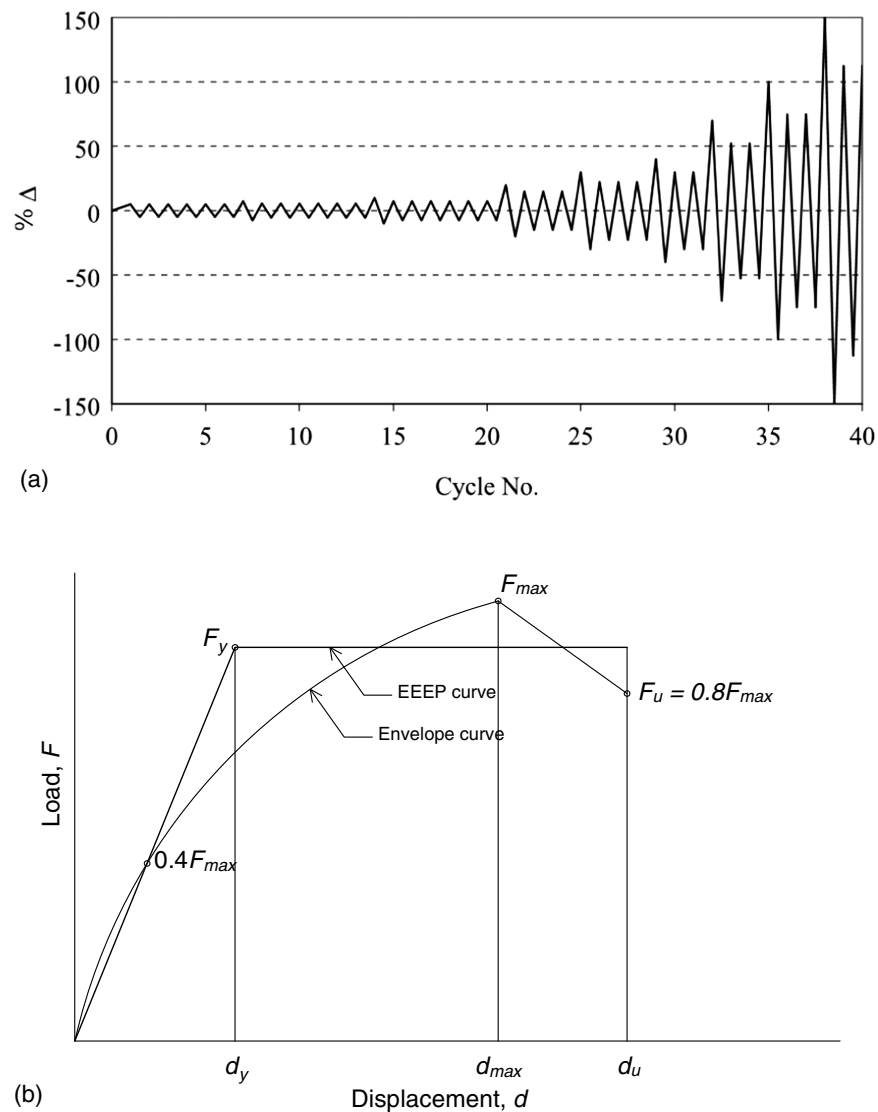


Fig. 5. (a) CUREE loading; and (b) equivalent energy elastic plastic (EEEE) curves (ASTM E2126).

tests are plotted in Figs. 7 and 8, respectively. The displacements are the horizontal displacements at the top of the wall, based on the measurements from String Pot 1, as shown in Fig. 4(a), and the loads provided are the cumulative applied load from both actuators.

The load-displacement behavior under monotonic loading of the CLT shear walls using the four different ledgers was similar (Fig. 7). The load-deflection curves were initially linear up to 10% of peak loads, and then the nonlinearity began due to deformations at the wall-to-floor and wall-to-wall joints. A sudden drop in actuator loads was observed when the spline connection reached its load-carrying capacity, which caused large HD deformation and triggered the failure.

The peak loads under monotonic loading F_{max} for the shear walls ranged from 115 (Type C—steel ledger with pin at center) to 133 kN (Type D wood ledgers with distributed screws). Shear walls with Type C ledgers had 11%, 6%, and 14% lower strength capacity compared to shear walls with type A, B, and D ledgers, respectively. The walls reached their peak loads at displacements of between 108 (Type A) and 129 mm (Type C); Type C shear-walls had 16%, 9%, and 5% greater deformation at ultimate capacity compared to shear walls with type A, B, and D ledgers, respectively. Shear walls with Type C ledgers reached the lowest

load-carrying capacity and highest corresponding deformation, confirming the assumption that the pins allowed the wall panels to rock freely with minimal restraint. All walls were deemed to have failed at loads F_u between 92 and 106 kN for ledger Types C and D, respectively. The shear wall with Type A ledger exhibited the largest displacement, at failure of 141 mm, whereas the Type C ledger failed at 133 mm.

Based on the EEEP curves, the yield loads from monotonic tests were 109 and 92 kN for the walls with ledger Types D and C, respectively. These obtained values were in good agreement with the predicted yield strength based on manufacturer values of 106 kN. The balloon walls yielded at an average displacement of 42 mm, ranging from 38 (Type B) to 46 mm (Type C). The monotonic tests showed these predicted values to be sufficiently accurate. All walls with screwed ledgers (Type A, B, and D) exhibited similar elastic stiffness (average $K_e = 2.5$ kN/mm). The Type C wall exhibited the lowest stiffness and smallest energy dissipation capacity compared with 10%, 15%, and 19% lower stiffness under cyclic tests when compared to Types A, B, and D, respectively and 25%, 17%, and 15% lower energy dissipation compared to Types A, B and D, respectively. These differences supported the hypothesis that the pin-connected ledger contributed little to resistance and allowed the



Fig. 6. Setup for ledger tests.

Table 1. Main results from shear wall tests

Test ID	$F_{\max+}$ (kN)	$F_{\max-}$ (kN)	$d_{F_{\max+}}$ (mm)	$d_{F_{\max-}}$ (mm)	E (kJ)	K_e (kN/mm)	F_y (kN)	d_y (mm)	F_u (kN)	d_u (mm)	D
A-M	129	—	108	—	—	2.5	107	42	103	141	3.3
A-C1	121	-101	112	-91	74	2.5	94	37	87	159	4.3
A-C2	117	-112	88	-95	71	2.7	96	35	90	177	5.0
B-M	122	—	117	—	—	2.6	100	38	97	140	3.7
B-C1	100	-99	111	-115	66	2.8	83	30	79	166	5.6
B-C2	106	-97	90	-90	65	2.7	85	31	78	176	5.6
C-M	115	—	129	—	—	2.0	92	46	92	133	2.9
C-C1	86	-95	89	-121	53	2.3	72	32	69	170	5.3
C-C2	97	-90	117	-93	56	2.4	79	33	74	177	5.3
D-M	133	—	123	—	—	2.5	109	43	106	135	3.1
D-C1	115	-103	116	-93	64	3.1	87	28	82	139	4.6
D-C2	104	-97	88	-94	64	2.7	86	32	80	150	4.7

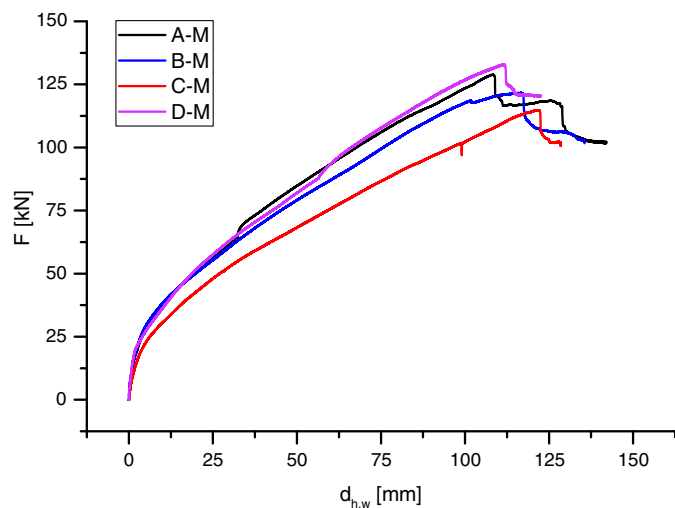


Fig. 7. Load-deflection curves for monotonic tests.

panels to rock freely. The lower overall lateral stiffness and energy dissipation triggered failure of the dissipative connections (HDs and panel-to-panel joints) at lower load levels. The ductility ratio D varied from 2.9 to 3.7, with the walls with Types B and C ledgers showing the highest and lowest ductility, respectively.

Under reversed cyclic loading, the peak loads F_{\max} of all shear walls was reduced compared to the monotonic tests. Walls with

Types C and D ledgers showed the highest F_{\max} reduction (21% and 20%, respectively) for both positive and negative hysteresis cycles. Walls with Type A ledgers showed the smallest average F_{\max} reduction of 7% and 17% in the positive and negative cycles, respectively. The deformations at maximum loads $d_{F_{\max}}$ were significantly reduced compared to the monotonic tests by up to 21% (average of positive and negative cycles for wall Type C). Walls with Type A ledgers showed the smallest d_{\max} reduction of 11% (again, average of positive and negative cycles).

The cyclic yield displacements and strengths d_y and F_y were similar for all ledger types. Yield displacement d_y ranged from 28 (Type D) to 37 mm (Type A) and was on average 23% smaller than the monotonic yield displacements. The largest reduction was observed for Type D walls (30%), whereas Type A walls exhibited the smallest reductions (14%). The yield strength F_y ranged from 72 (Type C) to 96 kN (Type A) and was on average 16% smaller than the monotonic yield strength. The largest reduction was again observed for Type D walls (21%), whereas Type A walls exhibited the smallest reductions (11%). The elastic stiffnesses K_e under cyclic loading were very similar across all ledger types and higher (11% on average) than those obtained from the monotonic tests. Walls with Type B and C ledgers were found to be more ductile than those with Type A and D ledgers, similar to the monotonic tests.

Furthermore, under reversed cyclic loading, the ultimate loads F_u of all shear walls was reduced compared to the monotonic tests by on average 20%. The largest reduction was again observed for Type D walls (24%), whereas Type A walls exhibited the smallest reductions (11%). The corresponding ultimate displacements d_u ,

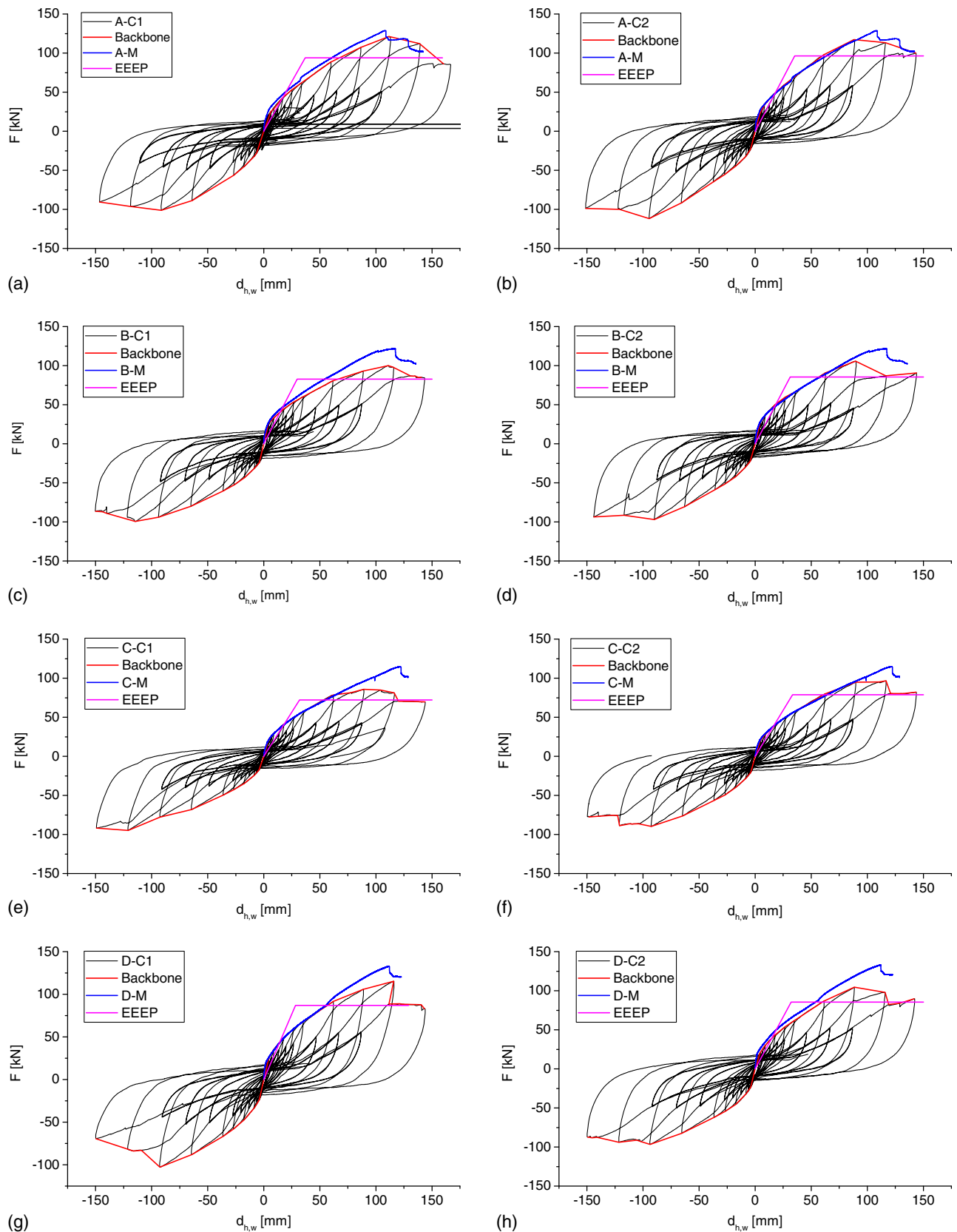


Fig. 8. Hysteresis curves: (a and b) Type A; (c and d) Type B; (e and f) Type C; and (g and h) Type D.

however, increased by an average of 20%. Here the largest increase was observed for Type C walls (30%), whereas the smallest increase was observed for Type D walls (7%). As a consequence of the decrease in d_y and increase in d_u , ductility increased for all

shear walls in the cyclic tests compared to the monotonic tests, with average values ranging from 4.7 (Type A and D walls) to 5.6 (Type B walls). Shear walls with ledger Type A achieved the highest energy dissipation capacity E , with 73 kJ, 25% higher

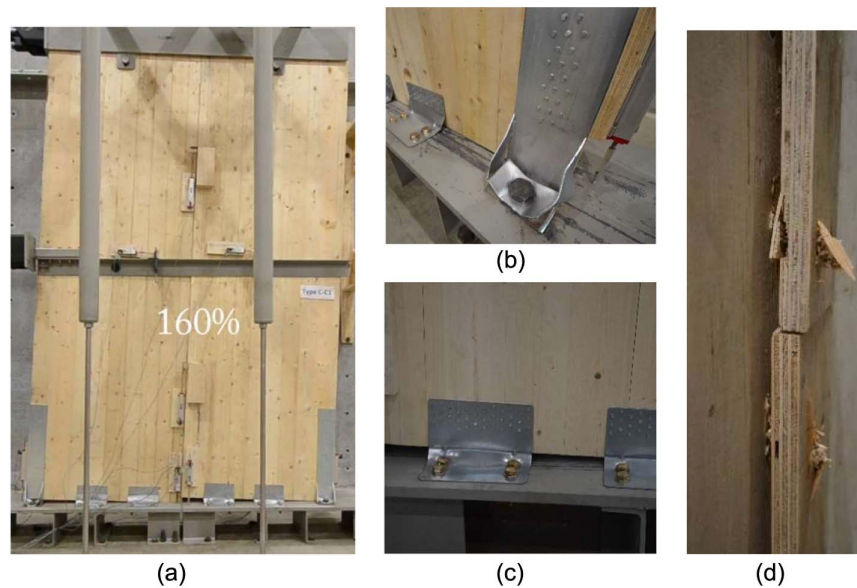


Fig. 9. (a) Shear wall after test, failure at (b) hold-down; (c) brackets; and (d) spline joints.

compared to the lowest energy dissipating capacity, observed in walls with Type C ledgers.

Shear Wall Failure Modes

At failure, all shear wall specimens showed fastener yield in the brackets and HDs [see Figs. 9(a–c)], failure of the spline joints [Fig. 9(d)], and plastic deformation of the horizontal steel plates for both HDs and brackets [Figs. 9(b and c)]. Under both monotonic and reversed cyclic loading, no damage was observed in either the steel or the wood ledgers.

Shear Wall Tests Secondary Results

The recorded shear wall uplift ($d_{up,w}$), sliding ($d_{sl,w}$), ledger movement relative to the panel ($d_{sl,l}$), and vertical slip between panels ($d_{z,p}$) at system failure (F_u) are summarized in Table 2 and illustrated in Figs. 10–13.

Fig. 10 shows the left corner of the right panels' uplift measured with LVDT 6. All shear walls under monotonic loading exhibited similar uplifts for all ledger types with values between 33 (Type D) and 41 mm (Type A). Cyclic tests showed uplifts on average approximately 15% larger, with a similar distribution between

ledger types. The panel uplifts at failure were on average 39 mm during monotonic testing and on average 44 mm during reversed cyclic testing.

Fig. 11 shows the horizontal sliding of the right panel for each test measured with LVDT 4. The horizontal panel sliding at failure during monotonic testing was negligible, with on average 1.1 mm, which represented less than 1% of the observed horizontal movement of the top of the wall (d_u). Under reversed cyclic testing, however, sliding increased to an average of 1.9 mm in the positive cycles and 6.0 mm in the negative cycles (after failure). From these observations, it can be concluded that the shear brackets effectively remained elastic and that panel rocking dominated the behavior of the shear wall system.

Fig. 12 illustrates the relative horizontal displacement between the ledgers and the right CLT panel measured with LVDT 9. The slips observed for all tests were very small; at relative failure, these ranged from around 0.8 mm for ledgers with nails distributed along their length (Types A and D) to around 3.1 mm for ledgers attached with grouped nails or with a pin at the centre of the panel (Types B and C). There was no real difference in ledger slips when comparing the results from the monotonic tests to those from the cyclic tests.

Table 2. Deformations at failure: shear wall uplift ($d_{up,w}$), shear wall sliding ($d_{sl,w}$), ledger relative displacement ($d_{sl,l}$), and panel-to-panel slip ($d_{z,p}$)

Test ID	$d_{up,w}$		$d_{sl,w}$		$d_{sl,l}$		$d_{z,p}$	
	Left panel	Right panel	(+)	(–)	(+)	(–)	(+)	(–)
	(mm)	(mm)	(mm)	(mm)	(mm)	(mm)	(mm)	(mm)
A-M1	44	41	1.4	—	0.3	—	48	—
A-C1	55	50	2.0	–8.4	0.8	–1.0	58	–41
A-C2	45	40	1.9	–5.6	1.0	–0.2	47	–45
B-M1	42	40	0.8	—	2.8	—	48	—
B-C1	45	42	2.2	–6.6	3.0	–2.5	50	–49
B-C2	45	41	1.9	–5.9	3.9	–3.0	50	–48
C-M1	38	37	1.1	—	2.4	—	36	—
C-C1	44	43	1.8	–3.3	3.7	–3.0	53	–50
C-C2	43	44	3.1	–6.9	2.7	–4.2	53	–51
D-M1	38	33	1.2	—	0.8	—	39	—
D-C1	43	42	0.4	–5.6	1.0	–1.3	50	–49
D-C2	45	38	1.8	–5.8	0.7	–1.5	45	–49

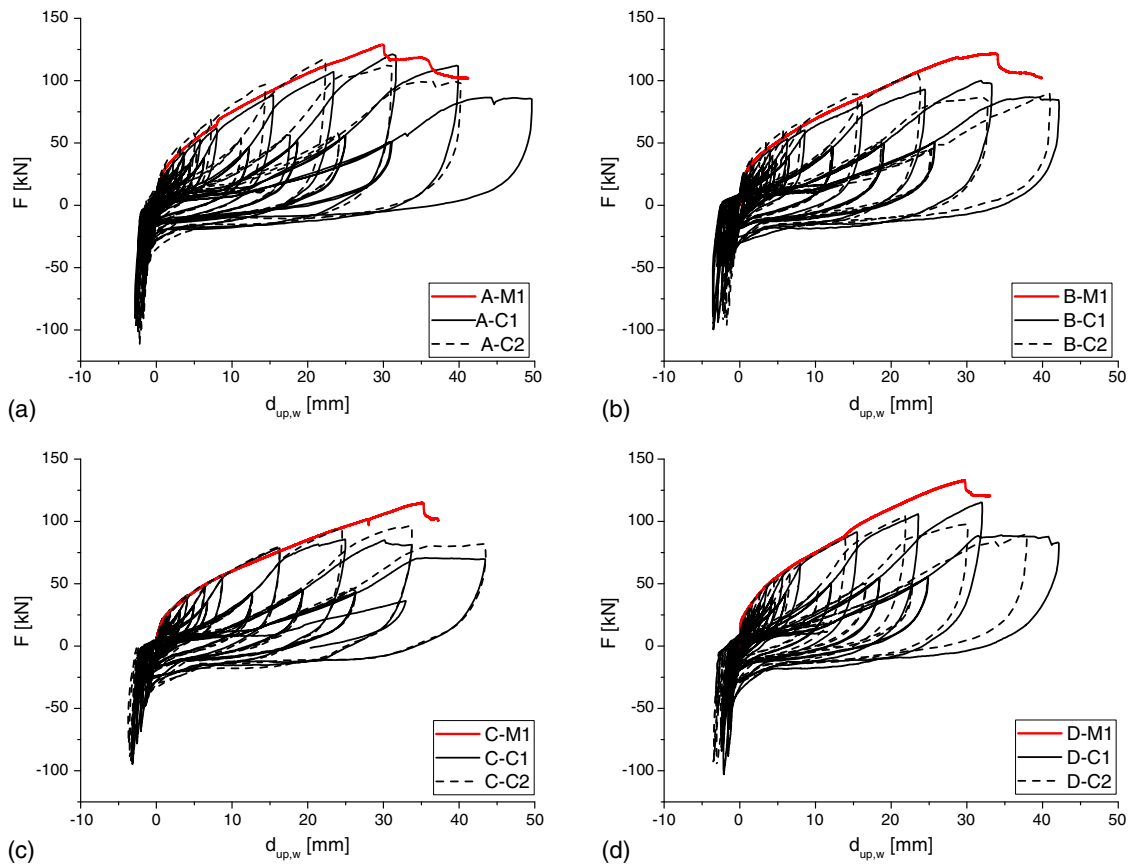


Fig. 10. Uplift of wall panels: (a) steel ledger Type A; (b) Type B; (c) Type C; and (d) wood ledger Type D.

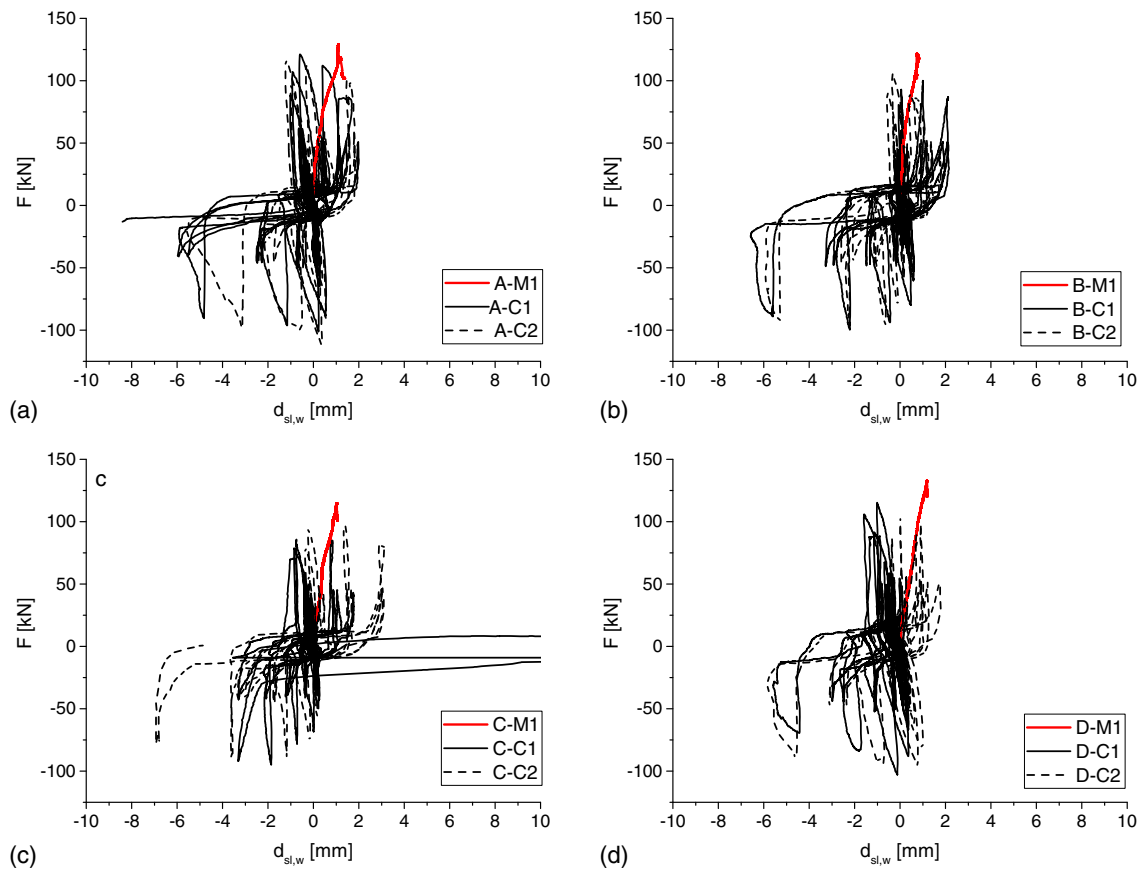


Fig. 11. Sliding of wall panel: (a) steel ledger Type A; (b) Type B; (c) Type C; and (d) wood ledger Type D.

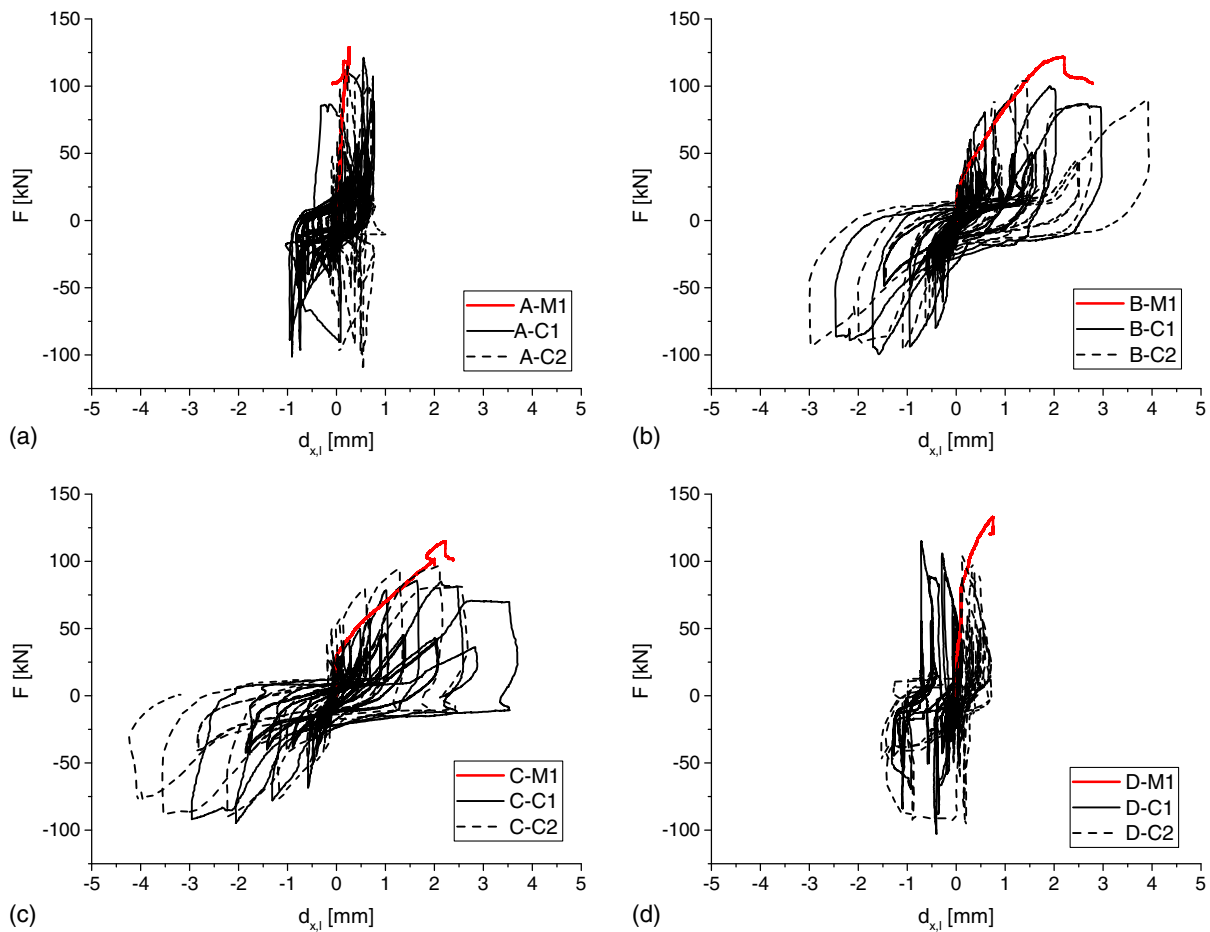


Fig. 12. Ledger relative slip: steel ledger (a) Type A; (b) Type B; (c) Type C; and (d) wood ledger Type D.

Fig. 13 shows the relative slips between the two coupled CLT panels measured at the center of the upper floor level with LVDT 12. The magnitudes and hysteresis behavior of the panel's relative slips (Fig. 13) and the lateral wall displacement (Fig. 8) measured at the top of the panel were similar. Hence, the relative slips between the two CLT panels corresponded well to the panel horizontal displacements at the top of the shear walls, supporting the assumption that the panels underwent a rigid body movement.

The slips between panels for shear walls with ledger Types A and B were found to be similar from monotonic and cyclic tests. However, for shear walls with ledger Types C and D, an increase in relative displacements of 30% and 19% was observed, respectively. The relative slip in the Type C wall was the lowest when tested under monotonic loading because the wall failed at much lower loads compared to other three types of walls. However, under cyclic loading, the relative slip of the panels in the Type C wall was found to be the highest, with averages of 53 and 50 mm in positive and negative cycles, although the walls failed at lower loads compared to other types of walls. The relative slips between panels were found to be on average 4 mm larger than the corner uplift values at failure. This is due to the vertical compression of the CLT panels at their corners, which was found to be between 3 and 5 mm; see Table 2.

Shear Wall Interstory Drifts

From the tests, the interstory drifts of the shear walls were estimated based on the maximum force (F_{max}) and corresponding

displacement (d_{Fmax}) observed at the floor levels as the ratio of each story drift (difference between top and ledger as well as ledger and bottom) and the floor height. The interstory drifts at top of the shear walls under monotonic loading were 3.2%, 3.4%, 3.5%, and 3.2% for shear walls with ledger Types A, B, C, and D, respectively. Under cyclic loading, these values decreased to 2.8%, 2.8%, 3%, and 2.8%; see Fig. 14. The results showed that the tested CLT balloon-framed shear walls could undergo the story drift limit required in NBCC (2020a) and ASCE 7 (ASCE 2017) of 2.5% with failing.

Ledger Tests

After the reversed cyclic shear wall tests were completed, one each of the ledger Types A (steel ledger with distributed screws), B (steel ledger with concentrated screws), and D (wood ledger with distributed screws) was tested under monotonic loading to failure to determine the remaining load-carrying capacity (postseismic tests). The results from the postseismic tests were compared against the new ledger tests of the same type, where each ledger was tested on a clean piece of CLT without experiencing any prior loading. The peak loads F_{max} and deformations d_{Fmax} were measured, and elastic stiffness K_e was determined for each test. The results from the ledger tests are listed in Table 3, and the corresponding load-deflection curves are plotted in Fig. 15. The three "new" ledgers reached load-carrying capacities from 254 (Type D) to 271 kN (Type B). The load-carrying capacities of the postseismic ledgers showed a small reduction

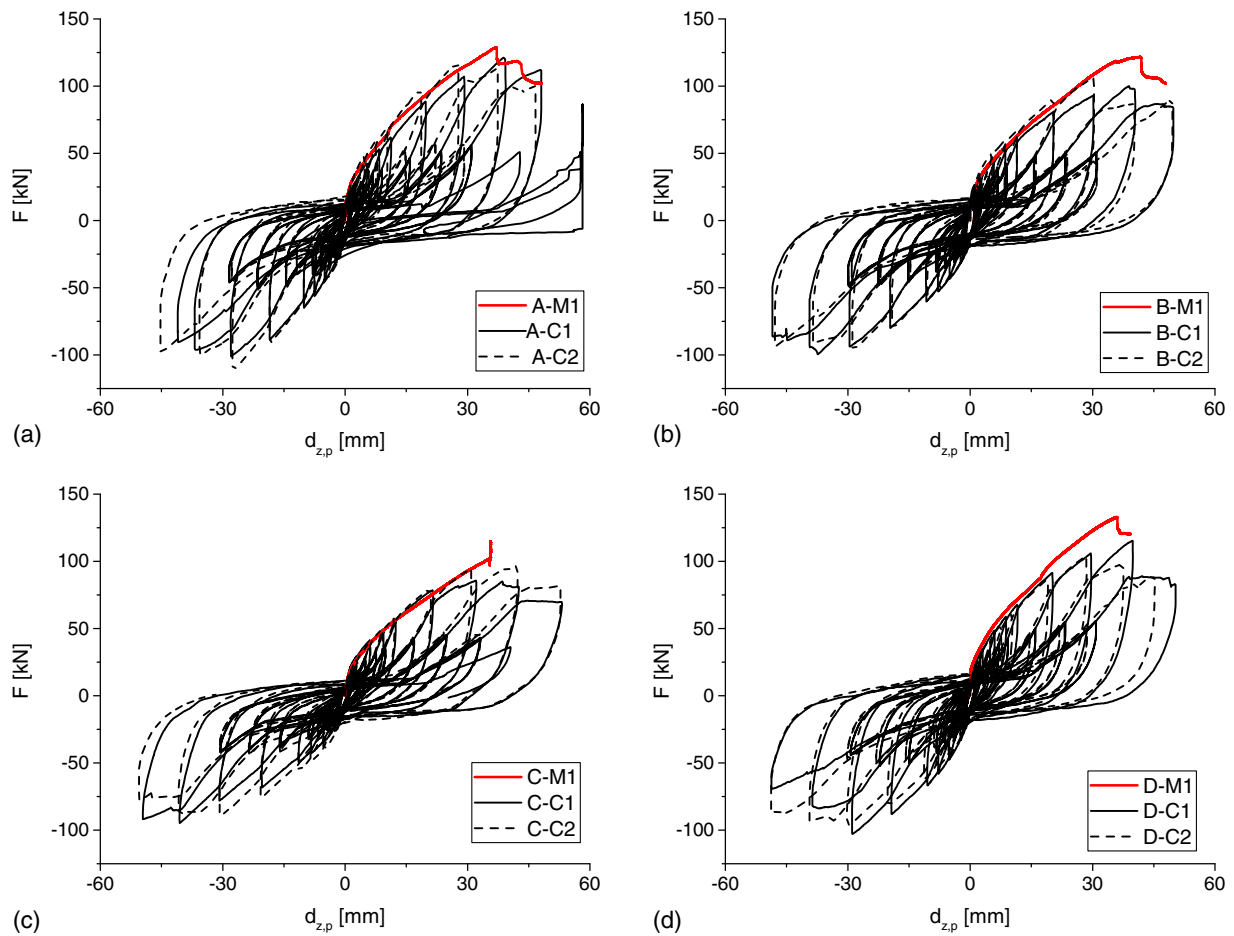


Fig. 13. CLT panel relative slip: steel ledger (a) Type A; (b) Type B; (c) Type C; and (d) wood ledger Type D.

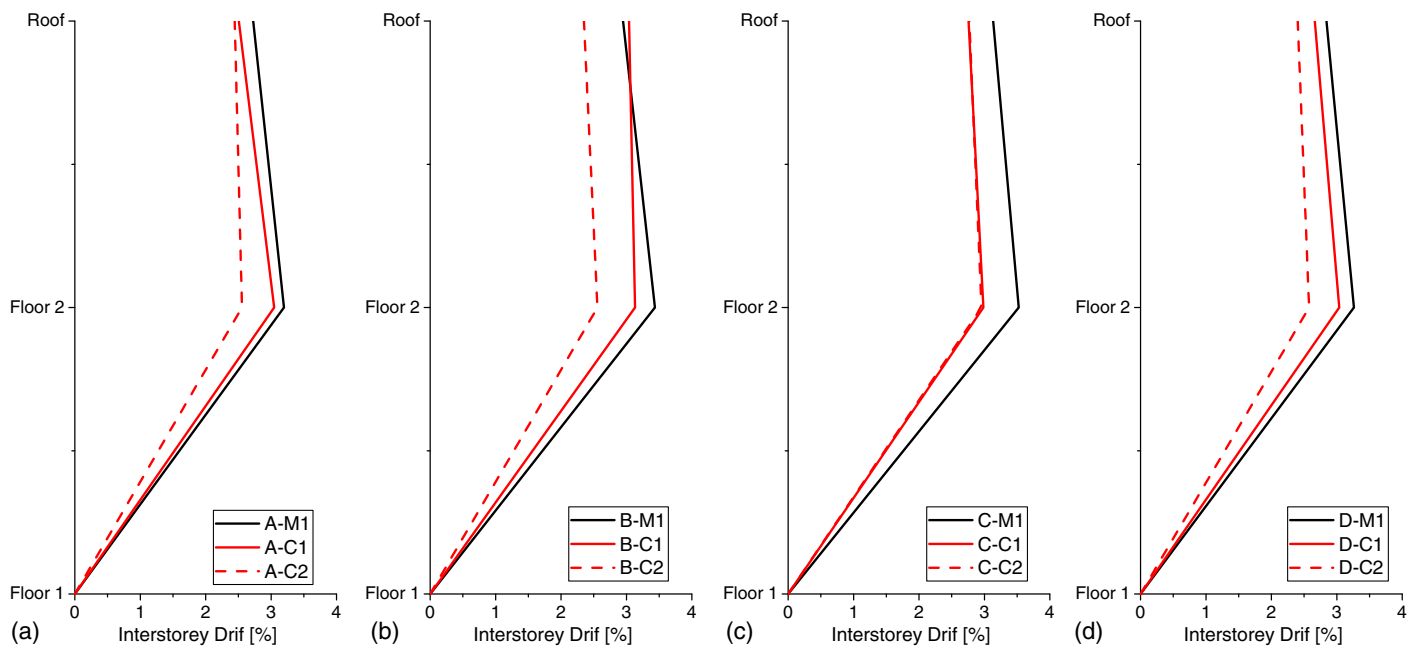


Fig. 14. Interstorey drifts: steel ledger (a) Type A; (b) Type B; (c) Type C; and (d) wood ledger Type D.

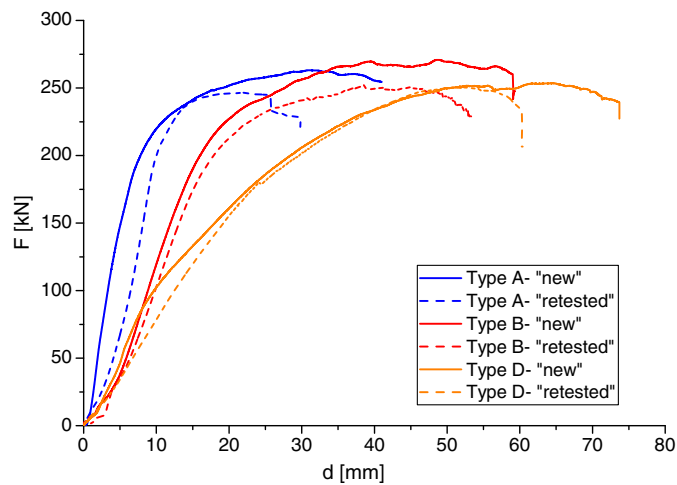
in strength of 7% (Type B) and 6% (Type A) and a minimal reduction of 1% (Type D).

The deformation at failure varied significantly, with the greatest variation between the new and postseismic ledgers occurring for

ledger Type A (8.8 mm or 29% reduction) and the lowest variation for ledger Type D (12.2 mm or 19% reduction). The reduction can be explained by assuming that a portion of the fasteners' plastic deformation capacity had been used due to the cyclic movement

Table 3. Ledger gravity test results

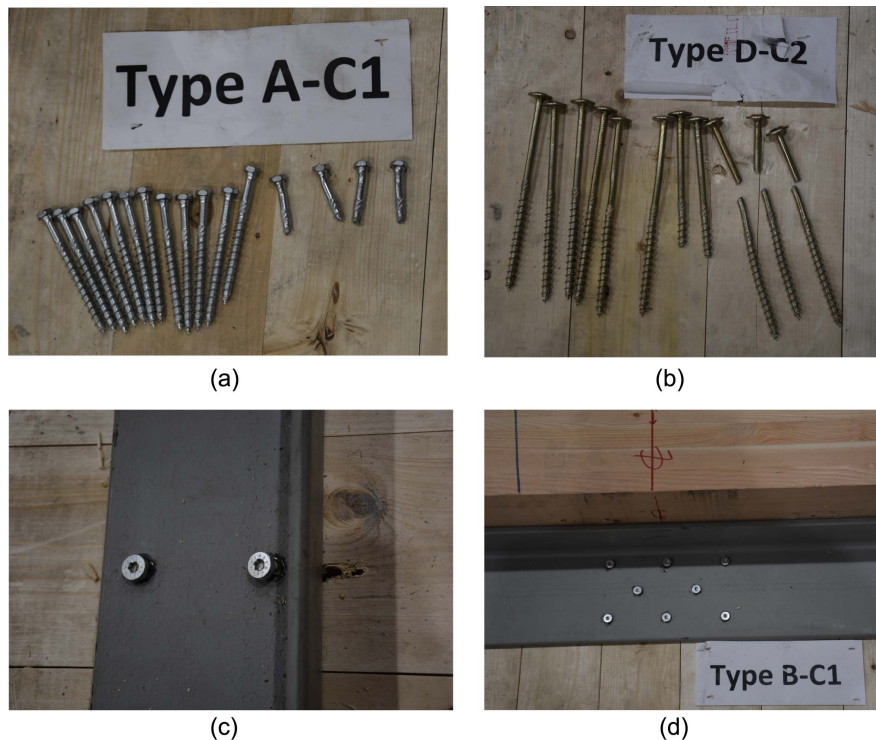
Ledger type	Tests	F_{max}		d_{Fmax}		K_e	
		(kN)	Δ (%)	(mm)	Δ (%)	(kN/mm)	Δ (%)
A	New	263	—	31	—	30	—
	Postseismic	247	-6	22	-29	15	-49
B	New	271	—	49	—	12	—
	Postseismic	252	-7	39	-21	10	-12
D	New	254	—	65	—	10	—
	Postseismic	251	-1	53	-19	8	-22

**Fig. 15.** Load-deflection curves from ledger tests.

of the panel relative to the ledger, particularly near the panel edges.

The elastic stiffness varied widely between the different ledger types. Type A exhibited the highest stiffness; the “new ledgers” reached 30 kN/mm, compared to only 12 and 10 kN/mm for ledger Types B and D, respectively. Ledger Type A in the “post-seismic” condition also exhibited the highest stiffness, 15 kN/mm, compared to only 10 and 8 kN/mm for ledger Types B and D, respectively. However, Type A also suffered the largest reduction in stiffness of 49% from “new” to “postseismic.” This can be explained by accounting for the initial deformation most likely to have occurred in the localized crushing at the fasteners due to vertical movement of the panels relative to the ledger, which is most intense for the ledgers with fasteners near the panel edge.

The observed failure mechanisms in all ledger tests was shown to be shearing of the screw fasteners, shown in Fig. 16. In general, it appears that the strength of the ledgers was unaffected, and the overall behavior of the ledgers remained a ductile mechanism regardless of ledger type.

**Fig. 16.** Shear failure (a) ASSYS Kombi screws in Type A shear walls; (b) ASSYS SK screws in Type D shear walls; failure of (c) Type A; and (d) Type B ledgers.

Conclusions

In this study, the lateral performance of 2-story balloon-frame CLT shear walls was tested under quasistatic monotonic and reversed cyclic loading. Four different types of ledger assemblies were evaluated: Types A (steel ledger with distributed screws), B (steel ledger with concentrated screws at centre), C (steel ledger with pin at centre), and D (wood ledger with distributed screws). In addition, six tests were conducted to investigate the ledgers' remaining load-carrying capacity after reversed cyclic loading. The following conclusions can be drawn:

1. Under monotonic loading, all four ledger types reached similar load-carrying capacities (115–133 kN), with Type D being the strongest. The four shear walls also reached similar deformations ($d_{F_{\max}} = 108\text{--}129$ mm), with Type C deforming the most. All walls had similar elastic stiffness K_e of around 2.5 kN/mm and similar ductility of between 2.9 and 3.1.
2. Under reversed cyclic loading, F_{\max} was substantially reduced by up to 21% (Type C). In parallel, the values of $d_{F_{\max}}$ also decreased by up to 17%. The elastic stiffness and ductility of all types of shear walls increased when compared to monotonic loading.
3. The tests confirmed the design assumptions based on elastic analysis for the Type A ledger (106 kN and 101 mm), where the contribution of the ledger was ignored. The cyclic tests showed these estimated values to be sufficiently accurate when compared to the Type C wall (92 kN and 105 mm), where the ledger's contribution was minimized by allowing fully rocking behavior.
4. Individual rocking of the coupled panels was the predominant kinematic mode, with the ratio between relative slip between panels and panel top displacement confirming rigid body movement. Sliding of the panels was low, relative slips between ledger and panels were negligible, and the horizontal component of the shear bracket behavior and ledger connection remained elastic for the duration of the tests, meeting the CSA-O86 capacity protection requirements.
5. Retesting the ledgers after undergoing reversed cyclic loading in the shear, all tests showed only a small loss in load-carrying capacity of between 1% for Type D and 7% for Type B. The cyclic loading on the system overall did not compromise the gravity strength of the ledger.
6. Overall, the differences between the four ledger types were small; the ledgers with distributed screws along their length (Types A and D) did not impede individual panel rocking, and when they did dissipate more energy, their ductility was comparable to the ledger using a perfect pin. Any of the tested ledgers was deemed suitable for implementation in the structural system.
7. The results obtained from this testing program show that a 2-story balloon-framed wall system appears to meet the design demands from CSA-O86. The results of these tests will be used in the design of a balloon-framed CLT school building in Vancouver, BC.

Data Availability Statement

Some or all data, models, or code that support the findings of this study are available from the corresponding author upon reasonable request.

Acknowledgments

The project was supported by Natural Resources Canada (NRCAN) through the Green Construction through Wood (GCWood) Program.

The support by UNBC technicians Michael Billups and Ryan Stern and undergraduate research assistant Anthony Bilodeau is greatly appreciated.

References

- ASCE. 2017. *Minimum design loads and associated criteria for buildings and other structures*. ASCE7-16. Reston, VA: ASCE.
- ASSY Kombi. 2020. "Hexagonal head partially threaded self-tapping structural wood screw." Accessed July 24, 2020. <https://mtcsolutions.com>.
- ASTM. 2011. *Standard test methods for cyclic (reversed) load test for shear resistance of walls for buildings*. ASTM E2126-11. West Conshohocken, PA: ASTM.
- BSI (British Standards Institution). 2004. *Eurocode 5: Design of timber structures. Part 1: General—Common rules and rules for buildings*. EN 1995-1-1. London: BSI.
- Cavanagh, T. 1997. "Balloon houses: The original aspects of conventional wood-frame construction re-examined." *J. Archit. Educ.* 51 (1): 5–15. <https://doi.org/10.1080/10464883.1997.10734741>.
- CEN (European Committee for Standardization). 1991. *Timber structures—Joints made with mechanical fasteners—General principles for the determination of strength and deformation characteristics*. EN 26891. Brussels, Belgium: CEN.
- Chen, Z., and M. Popovski. 2019. "Mechanics-based analytical models for balloon-type cross-laminated timber (CLT) shear walls under lateral loads." *Eng. Struct.* 208 (Apr): 109916. <https://doi.org/10.1016/j.engstruct.2019.109916>.
- CrossLam. 2020. "CrossLam CLT technical design guide." Accessed July 24, 2020. <https://www.structurlam.com>.
- CSA (Canadian Standards Association). 2019. *Engineering design in wood*. CSA Standard O86-19. Toronto: CSA.
- Daneshvar, H., J. Niederwestberg, C. Dickof, J. P. Letarte, and Y. H. Chui. 2019. "Cross-laminated timber shear walls in balloon construction: Seismic performance of steel connections." In *Proc., Modular and Off-site Construction*, 405–412. Edmonton, AB, Canada: Univ. of Alberta Library.
- Gavric, I., M. Fragiaco, and A. Cecotti. 2015a. "Cyclic behavior of CLT wall systems: Experimental tests and analytical prediction model." *J. Struct. Eng.* 141 (11): 04015034. [https://doi.org/10.1061/\(ASCE\)ST.1943-541X.0001246](https://doi.org/10.1061/(ASCE)ST.1943-541X.0001246).
- Gavric, I., M. Fragiaco, and A. Cecotti. 2015b. "Cyclic behavior of typical screwed connections for cross-laminated (CLT) structures." *Eur. J. Wood Wood Prod.* 73 (2): 179–191. <https://doi.org/10.1007/s00107-014-0877-6>.
- Gavric, I., M. Fragiaco, and A. Cecotti. 2015c. "Cyclic behaviour of typical metal connectors for cross-laminated (CLT) structures." *Mater. Struct.* 48 (6): 1841–1857. <https://doi.org/10.1617/s11527-014-0278-7>.
- Hossain, A., I. Danzig, and T. Tannert. 2016. "Cross-laminated timber shear connection with innovative self-tapping screw assemblies." *J. Struct. Eng.* 142 (11): 04016099. [https://doi.org/10.1061/\(ASCE\)ST.1943-541X.0001572](https://doi.org/10.1061/(ASCE)ST.1943-541X.0001572).
- Hossain, A., M. Popovski, and T. Tannert. 2019. "Group effects for shear connections with self-tapping screws in CLT." *J. Struct. Eng.* 145 (8): 04019068. [https://doi.org/10.1061/\(ASCE\)ST.1943-541X.0002357](https://doi.org/10.1061/(ASCE)ST.1943-541X.0002357).
- ICC (International Code Council). 2021. *ICC international building code*. Falls Church, VA: ICC.
- Izzi, M., D. Casagrande, S. Bezzi, D. Pasca, M. Follesa, and R. Tomasi. 2018. "Seismic behaviour of cross-laminated timber structures: A state-of-the-art review." *Eng. Struct.* 170 (Sep): 42–52. <https://doi.org/10.1016/j.engstruct.2018.05.060>.
- Karacabeyli, E., and S. Gagnon. 2019. *Cross laminated timber (CLT) handbook*. Vancouver, Canada: FPInnovations.
- Loss, C., A. Hossain, and T. Tannert. 2018. "Simple cross-laminated timber shear connections with spatially arranged screws." *Eng. Struct.* 173 (Oct): 340–356. <https://doi.org/10.1016/j.engstruct.2018.07.004>.
- Mestar, M., G. Doudak, M. Caola, and D. Casagrande. 2020. "Equivalent-frame model for elastic behaviour of cross-laminated timber walls with

- openings." *Proc. Inst. Civ. Eng. Struct. Build.* 173 (5): 363–378. <https://doi.org/10.1680/jstbu.19.00057>.
- NBCC (National Building Code of Canada). 2020a. *National building code of Canada 2015, Canadian commission on building and fire codes*. Ottawa: National Research Council of Canada.
- NBCC (National Building Code of Canada). 2020b. *National building code of Canada 2020, Canadian commission on building and fire codes*. Ottawa: National Research Council of Canada.
- Popovski, M., J. Schneider, and M. Schweinsteiger. 2010. "Lateral load resistance of cross laminated wood panels." In *Proc., World Conf. on Timber Engineering*. Riva del Garda, Italy: Univ. of Graz.
- Pozza, L., A. Saetta, M. Savoia, and D. Talledo. 2018. "Angle bracket connections for CLT structures: Experimental characterization and numerical modelling." *Constr. Build. Mater.* 191 (Dec): 95–113. <https://doi.org/10.1016/j.conbuildmat.2018.09.112>.
- Rothoblass. 2020. "Angle brackets and plates for buildings." Accessed July 24, 2020. <https://www.rothoblaas.com>.
- Schneider, J., Y. Shen, S. F. Stiemer, and S. Tesfamariam. 2015. "Assessment and comparison of experimental and numerical model studies of cross-laminated timber mechanical connections under cyclic loading." *Constr. Build. Mater.* 77 (Feb): 197–212. <https://doi.org/10.1016/j.conbuildmat.2014.12.029>.
- Shahnewaz, Md., M. S. Alam, and T. Tannert. 2018. "In-plane strength and stiffness of cross-laminated timber shear walls." *Buildings* 8 (8): 100. <https://doi.org/10.3390/buildings8080100>.
- Shahnewaz, Md., Y. Pan, M. S. Alam, and T. Tannert. 2020a. "Seismic fragility of cross-laminated timber platform buildings." *J. Struct. Eng.* 146 (12): 04020256. [https://doi.org/10.1061/\(ASCE\)ST.1943-541X.0002834](https://doi.org/10.1061/(ASCE)ST.1943-541X.0002834).
- Shahnewaz, Md., T. Tannert, M. S. Alam, and M. Popovski. 2017. "In-plane stiffness of cross laminated timber panels with openings." *Struct. Eng. Int.* 27 (2): 217–223. <https://doi.org/10.2749/101686617X14881932436131>.
- Shahnewaz, Md., T. Tannert, and M. Popovski. 2019. "Resistance of cross-laminated timber shear walls for platform-type construction." *J. Struct. Eng.* 145 (12): 04019149. [https://doi.org/10.1061/\(ASCE\)ST.1943-541X.0002413](https://doi.org/10.1061/(ASCE)ST.1943-541X.0002413).
- Shahnewaz, Md., T. Tannert, and M. Popovski. 2020b. "Deflection of cross-laminated timber shear walls for platform-type construction." *Eng. Struct.* 221 (Oct): 111091. <https://doi.org/10.1016/j.engstruct.2020.111091>.
- Sprague, P. E. 1981. "The origin of balloon framing." *J. Soc. Archit. Historians* 40 (4): 311–319. <https://doi.org/10.2307/989648>.
- Sullivan, K., T. H. Miller, and R. Gupta. 2018. "Behavior of cross-laminated timber diaphragm connections with self-tapping screws." *Eng. Struct.* 168 (Aug): 505–524. <https://doi.org/10.1016/j.engstruct.2018.04.094>.
- Trutalli, D., L. Marchi, R. Scotta, and L. Pozza. 2019. "Capacity design of traditional and innovative ductile connections for earthquake-resistant CLT structures." *Bull. Earthquake Eng.* 17 (4): 2115–2136. <https://doi.org/10.1007/s10518-018-00536-6>.